MICROWAVE SPECTRUM OF METHYLMERCURY CHLORIDE: GAS-PHASE DETERMINATION OF THE ELECTRIC DIPOLE MOMENT AND ^{201}Hg QUADRUPOLE COUPLING

Christopher A. REGO and A. Peter COX
Department of Physical Chemistry, University of Bristol, Bristol BS8 1TS, UK

Received 29 June 1987

The nuclear quadrupole coupling constant of ^{201}Hg ($I=3/2$) has been determined for CH_3HgCl in the vapour by microwave spectroscopy. A value of $eQq(^{201}Hg) = -1025(3)$ MHz, along the axis of the symmetric top, has been determined for the vibrational ground state. An initial determination of the quadrupole coupling constant was made possible by radiofrequency pumping of the l-type doublets of the lowest bending mode, ν_8, for which $eQq(^{201}Hg) = -1016(6)$ MHz and the l-type doublet constant $q_8 = 2.90(1)$ MHz. $eQq(^{35}Cl)$ was confirmed to be $-42.2(2)$ MHz. The dipole moment of CH_3HgCl has been determined from Stark effect measurements in the ground state as 3.411(11) D.

1. Introduction

We report here the first determination of a gas-phase ^{201}Hg quadrupole coupling constant for covalently bound mercury. The mercury coupling has been determined in the gas phase for the van der Waals complexes HgHCl and HgHCN in pulsed nozzle experiments [1]. In these two cases the coupling at Hg ($I=3/2$) is very small, despite the large quadrupole moment, and is rather different from the present case. CH_3HgCl with its strong microwave spectrum and relatively small coupling at chlorine offers the best opportunity of determining the large ^{201}Hg coupling in the gas phase. Mercury-201 coupling constants have been obtained in the solid state for $HgCl_2$ [2] and dioxane complexes of $HgCl_2$ and $HgBr_2$ [3] by nuclear quadrupole resonance spectroscopy. An electron spin resonance study [4] has given similar information for the CH_2HgCl radical in the crystalline phase.

The microwave spectrum of CH_3HgCl was first reported by Gordy and Sheridan [5], who derived the chlorine nuclear quadrupole coupling constants and a partial substitution structure. A millimetre-wave study [6] gave improved centrifugal distortion data. Later Walls et al. [7] assigned the spectra of the enriched ^{13}C and deuterium species. However, there has been no systematic investigation of the transitions arising from the $CH_3{}^{201}HgCl$ species (13.2%) and only tentative reference made to ^{201}Hg coupling.

In the present work the ^{201}Hg coupling was first measured for the first excited state of the bending mode, ν_8, by radiofrequency pumping of the l-type doublet transitions. This provided a good prediction for the widely spread ground-state ^{201}Hg components. Direct pumping of the quadrupole sublevels was subsequently used to examine specific (K, F) components [8,9].

In addition, we report the determination of the dipole moment of CH_3HgCl, the first of a mercury compound in the gas phase. This was accurately measured by a new approach for Stark measurements in which composite Stark components were measured at very large displacements and under moderate resolution.

2. Experimental

Methylmercury chloride was prepared by condensing BCl_3 onto a sample of methylmercury bromide mounted in the glass inlet to the waveguide cell. The CH_3HgCl was pumped at room temperature

0 009-2614/87/$ 03.50 © Elsevier Science Publishers B.V.
(North-Holland Physics Publishing Division)

through a stainless-steel X-band Stark cell. The spectrometer was of the Hughes–Wilson type employing 100 kHz modulation.

Radiofrequency–microwave double resonance was used to measure the *l*-type doublets and also to modulate selectively portions of the ^{201}Hg quadrupole patterns in the ground vibrational state. The double-resonance experiments were carried out according to the method of Wodarczyk and Wilson [10]. A Marconi signal generator (TF 801D/1, 10–470 MHz) and rf amplifier (TF 2172, 5–10 W) were used to supply the radiofrequency pumping.

Stark effect were determined by applying a direct voltage shift to the base line of the 100 kHz modulation and measuring the line displayed in the field-off phase [11]. The direct voltage was precisely supplied by a Brandenburg power supply (472R) and checked with a Fluke 5080A digital multimeter.

Wide-band measurements were made using backward wave oscillator sources and *X*, *Y* recorder presentation, while high-resolution measurements used klystrons with oscilloscope presentation.

3. Results

The spectrum of CH_3HgCl is complicated by the large number of mercury isotopes and the chlorine quadrupole splittings. The magnitude of the mercury isotope shifts causes lines to be spread over about 30 MHz at $J=5\leftarrow4$, which under wide-band sweep conditions coalesce to form one broad line (fig. 1a). Chlorine-35 hyperfine components were measured under high resolution for a number of transitions giving $eQq=-42.2(2)$ MHz, in good agreement with the value previously reported [5].

A vibrational satellite series arising from the HgCl stretching mode, ν_4, can be seen to low frequency of the ground state in fig. 1a; however, the doubly degenerate bending mode, ν_8, lies under the ground-state absorption. Fig. 2 shows the upper *l*-type doublets for $J=9\leftarrow8$ of $\nu_8=1$ under radiofrequency–microwave double resonance (RFMW) conditions. The relative abundances of the mercury isotopes are apparent and the ^{201}Hg quadrupole components appear between the ^{200}Hg and ^{202}Hg ines. The *l*-type doublet spectra appeared strongly during RFMW experiments to observe $CH_3{}^{201}Hg^{35}Cl$ lines by rf pumping via the quadrupole sublevels of ^{201}Hg. The *l*-type doublets from $J=8\leftarrow7$ to $J=10\leftarrow9$ were measured under rf pumping conditions because they were largely obscured by ground-state lines under Stark modulation.

The observed frequencies of the *l*-type doublets are listed in table 1. These frequencies were fitted with the equation [12]

$$\nu^{\pm}=2B_8^*(J+1)-4D_J(J+1)^3\pm q_8(J+1)\,,$$

where q_8 is larger than Grenier-Besson's *l*-type doubling constant by a factor of 4. The spectroscopic constants thus obtained are shown in table 2.

For the *l*-type doublets, where $K=1$, the chlorine hyperfine components lie entirely within the line width, thus providing a good opportunity to measure the ^{201}Hg quadrupole components. The quadrupole energy for the *l*-type doublets is given by [13]

$$W_Q=eQq[3/J(J+1)-1\pm\tfrac{1}{2}\eta]f(I,J,F)\,,$$

where η is the asymmetry parameter of the electric field gradient and $f(I, J, F)$ represents Casimir's function. The ^{201}Hg components for both the upper and lower *l*-type doublets from $J=8\leftarrow7$ to $J=10\leftarrow9$ have been observed and the frequencies of the lines measured are listed in table 3, along with the fitted constant *eQq*. No asymmetry in the electric field gradient has been detected at the ^{201}Hg nucleus for ν_8 in the present measurements. However an upper limit of $|0.04|$ can be placed on η.

The quadrupole coupling constant for the ν_8 mode was expected to give a good prediction for the ground-state ^{201}Hg quadrupole splittings; information for other molecules [14,15] suggested that *eQq* would not vary a great deal between the ground vibrational state and the first excited bending mode.

In order to differentiate between the $CH_3{}^{201}HgCl$ lines and the multitude of other lines, RFMW was used to modulate selectively portions of the ^{201}Hg quadrupole patterns. 100 kHz source modulated radiofrequency was used to pump between quadrupole levels at either the upper or lower *J* state, via the electric dipole transitions $\Delta J=0$, $\Delta K=0$, and $\Delta F=\pm1$, and $\Delta J=\pm$, transitions used as signal. The pumping efficiency is proportional to K^2, which, allowing for the $(J+1)^2-K^2$ dependence of the microwave signal intensity, favours the study of intermediate *K* values. A further consideration is the

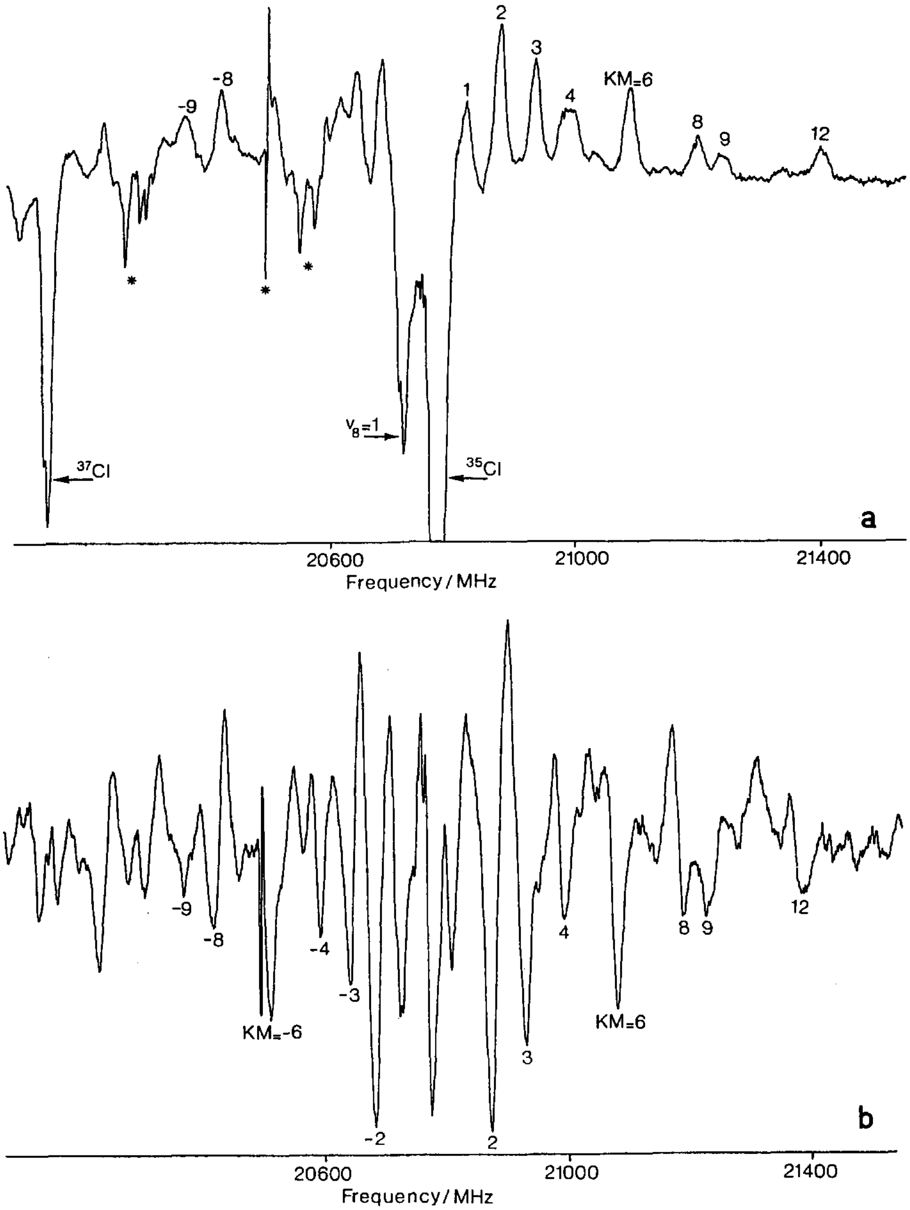

Fig. 1. Observed Stark effect for the $J=5\leftarrow4$ transition of CH_3HgCl. (a) Normal Stark modulation, $E=1771$ V cm^{-1}. Time constant = 300 ms, sweep rate = 2.4 MHz s^{-1}. * denote trace impurities of CH_3HgBr and HDO. (b) dc bias method; dc field = 1660.8 V cm^{-1}, ac field = 435 V cm^{-1}.

2:1 intensity enhancement due to nuclear-spin weighting for $|K|$ a multiple of three arising from the three equivalent protons in the CH_3 group.

An added complication in the assignment of $CH_3{}^{201}HgCl$ transitions is the effect of ^{35}Cl quadrupole coupling superimposed on each ^{201}Hg component. The best lines to study were ones in which the chlorine quadrupole collapsed into doublets. The measured frequencies are shown in table 4 along with *eQq* from a least-squares fit of the hypothetical centres of each ^{201}Hg component, taking into account the ^{35}Cl quadrupole interaction and the second-order

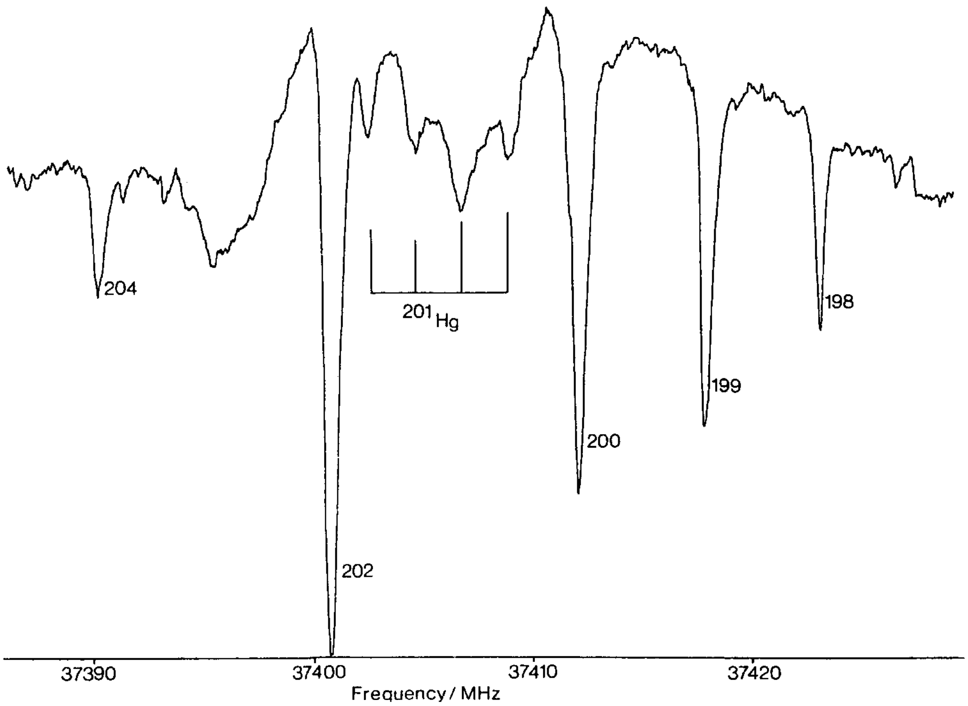

Fig. 2. Observed $J=9\leftarrow8$ upper l-type doublet transitions of the lowest degenerate vibration by radiofrequency–microwave double resonance (209 MHz rf pump). The $CH_3{}^{201}Hg^{35}Cl$ line is clearly split into four components. The calculated ^{201}Hg quadrupole pattern is shown in the stick diagram.

Table 1
Observed transition frequencies (MHz) for the l-type doublets in $v_8=1$ of the degenerate vibration ν_8 of $CH_3Hg^{35}Cl$

J' J''	Hg isotope	rf (MHz)	ν^+	$\Delta\nu$ (obs – calc)	ν^-	$\Delta\nu$ (obs – calc)
8 7	198	162	33265.52	−0.01	33218.86	−0.07
	199		33260.43	−0.04	33213.82	−0.06
	200		33255.40	−0.04	33208.86	0.01
	202		33245.46	0.01	33198.86	−0.01
	204		33235.56	−0.02	33188.96	−0.03
9 8	198	209	37423.46	0.02	37371.34	0.01
	199		37417.77	0.04	37365.65	0.03
	200		37412.05	−0.01	37359.95	0.00
	202		37400.81	−0.04	37348.76	0.02
10 9	198	262	41581.42	0.01	41523.53	0.05
	199		41575.09	−0.01	41517.13	0.01
	200		41568.83	0.03	41510.86	0.04
	202		41556.36	0.01	41498.37	0.00
	204		41544.07	0.06	41485.98	−0.04

[a] After correction for second-order quadrupole energies.

Table 2
Derived constants [a] for $CH_3Hg\,^{35}Cl$ for $v_8=1$

Hg isotope	B_8^* (MHz)	$B_0^0-B_8^*$ (MHz)
198	2077.670(10)	−0.187
199	2077.356(08)	−0.178
200	2077.042(10)	−0.178
202	2076.416(06)	−0.176
204	2075.800(10)	−0.18

J'	J''	q_8 (MHz)
8	7	2.912(4)
9	8	2.895(5)
10	9	2.899(5)

[a] Errors 1σ.

quadrupole coupling effects of the large mercury coupling. Some ^{201}Hg components were interfered with by strong *l*-type doublet lines which appeared due to off-resonance pumping and are not included in table 4.

Table 3
^{201}Hg quadrupole components (MHz) in $v_8=1$ of the degenerate vibration ν_8

J'	J''	F'	F''	Obs	$\Delta\nu$ (obs−calc) [a]
8	7	19/2	17/2	33253.89	−0.05
		17/2	15/2	33250.89	0.06
		13/2	11/2	33248.33	0.00
8	7	19/2	17/2	33207.56	0.03
		17/2	15/2	33204.36	−0.06
		13/2	11/2	33201.96	0.04
9	8	21/2	19/2	37409.22	−0.05
		19/2	17/2	37407.04	−0.04
		17/2	15/2	37402.66	0.04
		15/2	13/2	37404.79	0.05
9	8	21/2	19/2	37357.14	−0.01
		19/2	17/2	37354.96	0.00
		15/2	13/2	37352.62	0.01
10	9	23/2	21/2	41564.80	0.04
		21/2	19/2	41563.22	0.04
		19/2	17/2	41559.49	−0.06
		17/2	15/2	41561.05	−0.01
10	9	23/2	21/2	41506.84	0.04
		21/2	19/2	41505.23	0.01
		19/2	17/2	41501.46	−0.08
		17/2	15/2	41503.10	0.02

$eQq(^{201}Hg)=-1016\pm6$ MHz ($\pm\sigma$)

[a] After correction for second-order quadrupole energies.

4. Measurement of dipole moment

The dipole moment was determined from a Stark effect study of the $J=5\leftarrow4$ transition. A conventional high-resolution study of the Stark effect is difficult since the mercury isotopes and the superimposed chlorine quadrupole combine to make each Stark lobe about 20 MHz wide. However, to first order the Stark splitting is proportional to the product of K and M, and the low-resolution spectrum (fig. 1a) shows the Stark lobes corresponding to eight of the nine possible $+KM$ products for the $J=5\leftarrow4$ transition.

Final measurements were made using the dc bias method (fig. 1b) described in section 2. Both the $+KM$ and $-KM$ Stark components were measured, the frequency difference between these components cancelling any even-order effects in the Stark displacements and the effects of centrifugal distortion. Stark shifts up to 430 MHz have been measured using large Stark fields. The results, given in table 5 for the $KM=\pm2$, ±3 and ±6 components, have been analysed using a diagonalisation of the Stark-quadrupole matrix (truncated at $\Delta J\pm2$) [16].

5. Discussion

Radiofrequency–microwave double resonance has been the key to determining the quadrupole coupling for ^{201}Hg. The observation of the quadrupole components in the *l*-type doublet spectra gave the first experimental estimate of the ^{201}Hg coupling constant in CH_3HgCl. The *l*-type doubling constant q_8 (see table 2) agrees very well with the lowest bending mode ω_8 measured at 135 cm^{-1} in solution [17] and may be expressed as $q_8\approx2.7B_8^2/\omega_8$. The factor 2.7 is a very reasonable coefficient for the Coriolis summation in CH_3HgCl with two low stretching modes at 336 and 554 cm^{-1} [17].

Table 6 lists ^{201}Hg quadrupole coupling constants for comparison with that determined for gaseous CH_3HgCl. The other gas-phase value available [1] is for the van der Waals complex Hg...HCl. In that case the field gradient at the mercury nucleus is produced mainly by distortion of an otherwise spherical Hg configuration $(Xe)4f^{14}5d^{10}6s^2$ by the HCl molecule. The small $+ve$ coupling constant is quite well

Table 4
Hyperfine quadrupole components (MHz) for $CH_3{}^{201}Hg^{35}Cl$ in the ground vibrational state

rf (MHz)	J' J'' K	Obs	F'	F''	^{201}Hg derived component	$\Delta\nu$ (der−calc) [a]
25.7	6 5 3	24877.86 24875.46	13/2	11/2	24876.66	0.21
		24958.39 24956.01	9/2	7/2	24957.20	0.74
132	7 6 3	29045.84 29044.43	15/2	13/2	29045.14	−0.10
133	8 7 3	33234.78	19/2	17/2	33234.23	−0.02
		33233.68	13/2	11/2	33235.33	−0.01
87.1	8 7 5	33172.20 33169.74	17/2	15/2	33170.97	0.34
		33188.88 33186.20	15/2	13/2	33187.54	0.52
128.3	8 7 6	33174.75 33173.87 33171.08 33169.66	15/2	13/2	33172.29	0.01
		33148.11 33147.10 33144.17	17/2	15/2	37145.64	−0.13
160	9 8 3	37383.23	21/2 15/2	19/2 13/2	37383.23	0.01
128.3	9 8 6	37335.03 37332.12	17/2	15/2	37333.58	−0.08
		37397.02 37394.19	21/2	19/2	37395.61	0.06
42.8	10 9 5	41538.00 41536.10	21/2	19/2	41537.05	−0.51
		41543.20 41541.20	17/2	15/2	41542.20	0.10

$eQq(^{201}Hg) = -1025 \pm 3$ MHz($\pm\sigma$)

[a] Includes correction for second-order quadrupole energies. Centres of ^{201}Hg quadrupole pattern fixed using $B_0 = 2076.552$ MHz from our analysis, and $D_J = 0.25$ kHz, $D_{JK} = 21.0$ kHz from ref. [6].

described by a polarisation model allowing an estimate of the Sternheimer shielding factor. The other values in table 6 are very different, large and negative, and are more readily described in terms of sp hybridised orbitals on mercury. The coupling constant in $HgCl_2$ has been interpreted in terms of sp hybridisation with 60% ionic character in the HgCl bonds [2]. Using this model Gordy has derived a value for the coupling per p electron in the 6s6p configuration of Hg as −1000 MHz. On the same basis, CH_3HgCl (and indeed $\cdot CH_2HgCl$) would be expected to have a coupling constant of ≈ -880 MHz. The gas-phase value for CH_3HgCl suggests a larger magnitude for the coupling per p electron of −1165 MHz.

Table 5
Stark shift data for $J=5\leftarrow4$ transition ($v=0$) of $CH_3Hg^{35}Cl$

E (V/cm)	$\frac{1}{2}(\nu^+-\nu^-)$ (MHz)	$\Delta\nu^\pm$(obs−calc)	μ (D)
$\lvert KM\rvert=2$			
1087.5	61.90	−0.24	3.400(10)
1406.5	80.75	0.27	
1770.8	101.35	−0.15	
2367.4	136.35	0.10	
$\lvert KM\rvert=3$			
1406.5	121.10	−0.20	3.422(7)
1770.8	152.85	0.02	
2127.1	183.85	0.13	
2367.4	205.84	0.06	
$\lvert KM\rvert=6$			
1087.5	187.05	0.26	3.412(5)
1406.5	241.70	−0.01	
1770.8	304.30	−0.16	
2127.1	365.85	−0.06	
2367.4	407.40	−0.04	
$\mu_{av}=3.411(11)$ [a]			

[a] Error 1σ.

The magnitude derived previously from measurements on $HgCl_2$ in the solid state may be low because of $HgCl_2$ intermolecular contacts [18]. Strong complexing in the solid clearly lowers the Hg coupling constant as observed in the $HgCl_2(diox)_2$ case (see table 6 and ref. [3]). More recently [19] we have determined an even larger ^{201}Hg coupling constant for CH_3HgCN. Explanation of these larger values obtained for these linear gas-phase complexes of Hg may well need a departure from the traditional sp hybrid description. The use of d–s hybridisation in the bonding of these complexes has been suggested in an early paper by Orgel [20], and some d→π* contribution in CH_3HgCN has been deduced from photoelectron spectra [21]. We intend to measure further ^{201}Hg quadrupole coupling constants to help find a better bonding description of these linear complexes and perhaps deduce a more appropriate value for the atomic coupling for mercury.

The gas-phase dipole moment of CH_3HgCl (3.41 D) agrees quite well with solution values, 2.99 D in benzene and 3.06 D in dioxane [22]. These differences reflect the difficulty of applying the Debye method in solution for these complexes which have a low solubility in non-polar solvents.

Acknowledgement

We thank the SERC for a research studentship. We also thank Michael R. Edwards for assistance with this work.

References

[1] J.A. Shea and E.J. Campbell, J. Chem. Phys. 81 (1984) 5326.
[2] H.G. Dehmelt, H.G. Robinson and W. Gordy, Phys. Rev. 93 (1954) 480.
[3] D.B. Patterson, G.E. Peterson and A. Carnevale, Inorg. Chem. 12 (1973) 1282.
[4] C.M.L. Kerr, J.A. Wargon and F. Williams, J. Chem. Soc. Faraday Trans. II 72 (1976) 552.
[5] W. Gordy and J. Sheridan, J. Chem. Phys. 22 (1954) 92.
[6] J.T. Cox, T. Gäumann and W.J. Orville-Thomas, Discussions Faraday Soc. 19 (1955) 52.
[7] C. Walls, D.G. Lister and J. Sheridan, J. Chem. Soc. Faraday Trans. II 71 (1975) 1091.
[8] A.P. Cox, G. Duxbury, J.A. Hardy and Y. Kawashima, J. Chem. Soc. Faraday Trans. II 76 (1980) 339.

Table 6
Measured values of ^{201}Hg quadrupole coupling constants

Experimental method	Molecule	eQq (MHz)	Ref.
NQR	$HgCl_2$ (solid)	$\lvert 724\rvert$	[2]
NQR	$HgCl_2(diox)_2$ (solid)	$\lvert 646\rvert$	[3]
ESR	$\cdot CH_2HgCl$ (solid)	$\lvert 900\rvert$	[4]
microwave	CH_3HgCl (vapour)	−1025	present work
microwave	Hg.HCl (vapour)	5.993	[1]

[9] A.P. Cox, I.C. Ewart and T.R. Gayton, J. Mol. Spectry., to be published.

[10] F.J. Wodarczyk and E.B. Wilson, J. Mol. Spectry. 37 (1971) 445.

[11] A.P. Cox, I.C. Ewart and W.M. Stigliani, J. Chem. Soc. Faraday Trans. II 71 (1975) 504.

[12] M.L. Grenier-Besson and G. Amat, J. Mol. Spectry. 8 (1962) 22.

[13] H.E. Radford and C.V. Kurtz, J. Res. Natl. Bur. Std. 74a (1970) 791.

[14] R.L. Kuczkowski, J. Mol. Spectry. 45 (1973) 261.

[15] T. Chikaraishi and E. Hirota, Bull. Chem. Soc. Japan 46 (1973) 2314.

[16] G.L. Caldow, G. Duxbury and L.A. Evans, J. Mol. Spectry. 69 (1978) 239.

[17] P.L. Goggin, G. Kemeny and J. Mink, J. Chem. Soc. Faraday Trans. II 72 (1976) 1025.

[18] E.V. Bryuchova and G.K. Semin, J. Chem. Soc. Chem. Commun. (1972) 1216.

[19] C.A. Rego and A.P. Cox, to be published.

[20] L.E. Orgel, J. Chem. Soc. (1958) 4186.

[21] P. Burroughs, S. Evans, A. Hamnett, A.F. Orchard and N.V. Richardson, J. Chem. Soc. Chem. Commun. (1974) 921.

[22] T.Ya. Mel'nikova, Yu.V. Kolodyazhnyi, A.K. Prokof'ev and O.A. Osipov, Zh. Obshchei Khim. 46 (1976) 1820.